



**EFFECTS OF METALLIC  
NANOPARTICLES AS  
ANTIMICROBIALS OF  
NON-NEWTONIAN  
FLUID FLOW  
THROUGH DISEASED ARTERIES**

**UMAR BALA**

*Department of General Studies, Federal  
Polytechnic, Bauchi, PMB 0231, Bauchi State.  
Nigeria.*

**Abstract**

**T**he current investigation is the study of different types of nanoparticles such as copper (Cu), titanium (TiO<sub>2</sub>) and aluminum (Al<sub>2</sub>O<sub>3</sub>) in the existence of mild stenosis lesions. To account the gravitational effects artery is considered longways. The exact solutions are achieved by using the Euler–Cauchy method. The presented graphs show the thermophysical properties of fluids (blood) and nanoparticles through the velocity profile ( $V_z$ ), volume fraction ( $\phi$ ), Grashof number ( $Gr$ ), heat source or sink parameter ( $\theta$ ), resistance impedance ( $\lambda$ ), wall shear stress ( $\tau_{rz}$ ) and temperature profile ( $\vartheta$ ). The obtained results show that the transmission of axial velocity curves through a pure fluid ( $\phi=0$ ) is substantially lower at (-

$0.505 \leq r \leq 0.505$ ) than that through a nanofluid. The size of trapping bolus in the case of pure fluid flow ( $\phi=0$ ) is smaller than

**KEYWORDS:**

Homogenous  
flow model,  
Nanoparticles  
Blood flow  
Stenosis,  
Grashof number

that through nanofluid.

## INTRODUCTION

Coronary artery disease or stenosis is the important causal agent of death in various countries. There is a significant proof that vascular fluid mechanics play a key role in the progression and development of arterial stenosis, which is one of the most common diseases in mammals.

The mechanical study of blood flow in arteries allows some important aspects due to the feasible medical applications as well as the engineering interest. The hemodynamic nature of the blood flow is determined by the occurrence of the arterial atherosclerosis. The normal blood flow in the presence of coronary artery disease or stenosis in an artery is altered. The study of pulsatile flow through a stenosis is motivated by the need to get a fuller apprehension of the influence of flow phenomena on stroke and atherosclerosis. To realize the consequence of stenosis on blood flow through and beyond the section of the artery, many studies have been assumed theoretically and experimentally [1–3]. Plenty of investigations have been available to understand disorders in a blood flow that are due to stenosis by treating blood as a Newtonian or non-Newtonian fluid. Numerical solutions of pulsatile flow have been described by several investigators. Liu and Tang [4] discussed the viscous model in arteries with stenosis. They discussed the stenosis severity and flow rate from numerical results. Siegel et al. [5] discussed the wall shear rate through an arterial stenosis by assuming blood as a Newtonian fluid. Zamir [6] has given mathematical treatment in the blood flow in arteries subject to various physiological conditions. Several studies [7–9] discussed that the blood vessel walls may be movable, flexible and permeable and the theoretical investigations related to the non-Newtonian blood flow through stenosed arteries.

Ellahi et al. [10] discussed the blood flow model through composite stenosis. They treated blood as a micropolar fluid model under the mild stenosis case. Mekheimer and El Kot [11] discussed the micropolar fluid model for axis-symmetric blood flow through radially symmetric but axially nonsymmetric mild stenosis tapered arteries. Sankar and Lee [12] discussed the mathematical model of pulsatile flow of non-

Newtonian fluid in stenosed arteries. Here they discussed the Herschel Bulkley fluid and found an analytical solution by using a regular perturbation method. Ellahi et al. [13] designed the unsteady and incompressible flow of non-Newtonian fluid through composite stenosis. The micropolar fluid is treated as a blood flow model with mild stenosis and slip velocity is also taken into account.

Nanoparticles usually ranging in dimension from 1 to 100 nanometers (nm) have properties unique from their bulk equivalent. With the decrease in the dimensions of the materials at the atomic level, their properties change. The nanoparticles possess unique physicochemical, optical and biological properties which can be manipulated suitable for desired applications [14,15]. This investigation is concerned with the boundary layer flow of viscous nanofluid over a permeable stretching wall. The fluid saturates the porous medium. Four different types of nanoparticles such as copper (Cu), silver (Ag), alumina ( $Al_2O_3$ ) and titanium oxide ( $TiO_2$ ) with water as its base fluid are considered.

The nanoparticles are broadly grouped into organic and inorganic nanoparticles [16]. Magnetic field effect on CuO–water nanofluid flow and heat transfer in an enclosure which is heated from below is investigated.

The Lattice Boltzmann method is applied to solve the governing equations. The effective thermal conductivity and viscosity of nanofluid are calculated by the KKL (Koo–Kleinstreuer–Li) correlation. In this model the effect of Brownian motion on the effective thermal conductivity is considered [17]. In this study, the natural convection boundary layer flow along with inverted cone, magnetic and heat generation of water and ethylene glycol based nanofluids is considered by means of variable wall temperature [18]. Emerging infectious diseases and the increase in the incidence of drug resistance among pathogenic bacteria have made the search for new antimicrobials inevitable. In the current situation, one of the most promising and novel therapeutic agents is the nanoparticles. The unique phytochemical properties of the nanoparticles combined with the growth inhibitory capacity against microbes have led to the

upsurge in the research on nanoparticles and their potential application as antimicrobials [19].

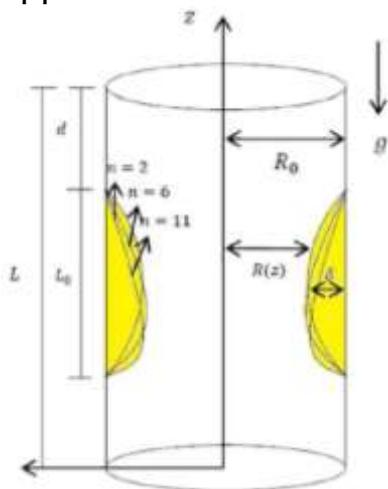


Fig. 1. Schematic diagram of stenosed artery.

Copper oxide (Cu) nanoparticles were characterized and investigated with respect to potential antimicrobial applications. It was found that nanoscaled (Cu), generated by thermal plasma technology, contains traces of pure (Cu) and (Cu<sub>2</sub>O) nanoparticles. Transmission electron microscopy (TEM) demonstrated particle sizes in the range 20 – 95 nm. TEM energy dispersive spectroscopy gave the ratio of copper to oxygen elements at 54.18% to 45.26%. The mean surface area was determined as 15.69 m<sup>2</sup>/g by the Brunauer–Emmett–Teller (BET) analysis. (Cu) nanoparticles in suspension showed activity against a range of bacterial pathogens, including meticillin-resistant *Staphylococcus aureus* (MRSA) and *Escherichia coli*, with minimum bactericidal concentrations (MBCs) ranging from 100 g/mL to 5000 g/mL. The ability of (Cu) nanoparticles to reduce bacterial populations to zero was enhanced in the presence of sub-MBC concentrations of silver nanoparticles. Studies of (Cu) nanoparticles incorporated into polymers suggest that the release of ions may be required for optimum killing [20].

The inhibitory activity of (TiO<sub>2</sub>) is due to the photocatalytic generation of strong oxidizing power when illuminated with UV light at a wavelength of less than 385 nm [21–23]. (TiO<sub>2</sub>) particles catalyze the killing of bacteria on illumination by near-UV light. The generation of

active free hydroxyl radicals ( $-OH$ ) by photoexcited ( $TiO_2$ ) particles is probably responsible for the antibacterial activity [24–26]. The antimicrobial effect of ( $TiO_2$ ) photocatalyst on *E. coli* in water and its photocatalytic activity against fungi and bacteria have been demonstrated [27–30].

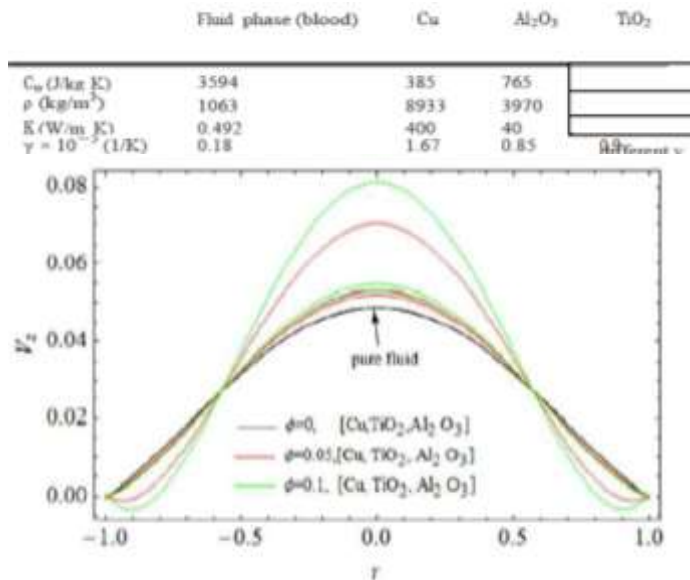


Fig. 2. Variation of velocity profiles  $V_z$  against  $r$  for different values of volume fraction  $\phi$  with  $\delta = 0.01, F = 0.01, d = 0.5, n = 2, z = 1.2, Gr = 0.8, \beta = 2.0$

Aluminum oxide NPs have wide-range applications in industrial and personal care products. The growth-inhibitory effect of alumina NPs over a wide concentration range ( $10\text{--}1000 \mu\text{g/mL}$ ) on *E. coli* has been studied. Fourier transform-infrared studies have shown differences in structure between nanoparticle treated and untreated cells. Alumina nanoparticles have exhibited a mild growth-inhibitory effect, only at very high concentrations. This is attributed to surface charge interactions between the particles and cells. It is possible that the free-radical scavenging properties of the particles might have prevented cell wall disruption and drastic antimicrobial action [31].

Nanoparticle study is now an active area of scientific interest due to wide applications in various fields like optical, electronic and biomedicine i.e. radiation therapy for cancer treatment, deliver drugs by targeting rotted arteries which have been developed as a

noninvasive method to contest heart disease, especially copper nanoparticles that correct abnormal heart enlargement called hypertrophic cardiomyopathy [32]. The nanofluid model was first developed by Choi [33] and after him highlighted by Gentile et al. [34] discussed longitudinal transport of nanoparticles in blood vessels by considering blood as Casson fluid.

Nadeem et al. [35] discussed the nanoparticle analysis of blood flow through tapered arteries and examined the hemodynamic effects due to stenosis.

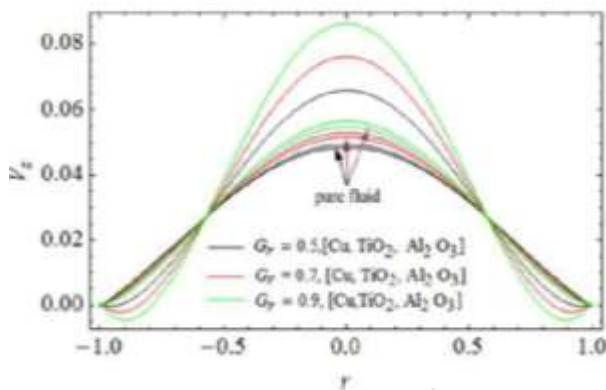


Fig. 3. Variation of velocity profiles  $V_z$  against  $r$  for alues of Grashof number  $Gr$  different  $v$  with  $\delta = 0.01, F = 0.01, d = 0.5, n = 2, z = 1.2, \varphi = 0.1, \beta = 2.0$ .

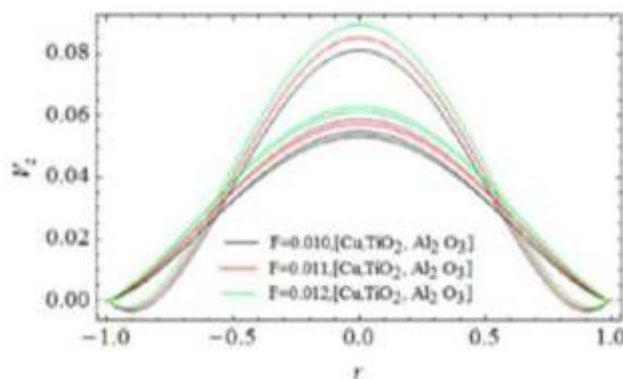


Fig. 4. Variation of velocity profiles  $V_z$  against  $r$  for different values of flow rate  $F$  with  $\delta = 0.01, Gr = 0.8, d = 0.5, n = 2, z = 1.2, \varphi = 0.1, \beta = 2.0$ .

Holding in perspective the importance of the above analysis in medicine, the purpose of the present article is to talk about the effects

of nanoparticles as an antimicrobial which are copper (Cu), titanium (TiO<sub>2</sub>) and aluminum (Al<sub>2</sub>O<sub>3</sub>) suspended in the base fluid (blood) through an artery (as shown in Fig. 1). According to the authors' knowledge this kind of study is not explored so far. Exact solution of the governing equations along with the boundary conditions of stenosed symmetric artery has been calculated. The expressions for velocity, temperature, resistive impedance, and wall shear stress at the stenosis throat have been examined.

## 2. Mathematical model

Consider unsteady, laminar and the incompressible viscous fluid in the presence of nanoparticles flowing through the artery having a finite length L with stenosis. Let (r, θ, z) be the coordinates of a material point in the cylindrical polar coordinate system where the z-axis is taken along the axis of the artery while r is taken along the radial and circumferential directions respectively. Further, we assume that (r=0) is chosen as the axis of the symmetry of the artery. The geometry of the arterial wall with stenosis model is defined by the function R(z), as in Fig. 1 can be written mathematically as [13].

$$R(z) = \begin{cases} R_0 \left[ 1 - \eta \left( \frac{z-d}{L_0} \right)^n \right] & ; \quad d \leq z \leq d + L_0 \\ R_0 & \text{otherwise} \end{cases}$$

The parameter  $\eta$  is given by

$$\eta = \frac{\delta R_0 L_0^{n-1}}{\rho \delta^{n-1}}$$

Fig. 5. Variation of velocity profiles Vz against r for different of values of heat source or sink parameter  $\beta$  with  $\delta = 0.01, F = 0.01, d = 0.5, n = 2, z = 1.2, \varphi = 0.1, Gr = 0.8$ .

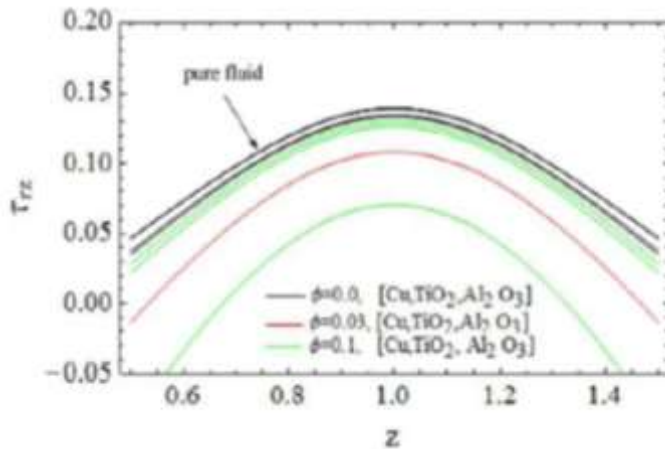


Fig. 6. Variation of the wall shear stress distribution  $\tau_{rz}$  with  $z$  for different values of volume fraction  $\phi$  with  $\delta = 0.2, F = 0.01, d = 0.5, n = 2, Gr = 0.8, \beta = 2.0$ .

where  $R_0$  is the constant radius of the normal artery in the non-stenotic region,  $L_0$  is the length of stenosis,  $d$  is the location of the stenosis,  $\delta$  is taken to be the severity of the stenosis, and ( $n \geq 2$ ) is the parameter determining the shape of the constriction profile and referred to the shape parameter (the symmetric stenosis occurs for  $n=2$ ).

The governing equations for conservation of mass, momentum and temperature of viscous fluid can be taken as:

$$\frac{\partial V_r}{\partial r} + \frac{V_r}{r} + \frac{\partial V_z}{\partial z} = 0; \quad (82)$$

$$\rho_{eff} \frac{\partial V_r}{\partial t} + \frac{\partial V_r}{r} + \frac{\partial V_z}{\partial z} = - \frac{\partial p}{\partial r} + \mu_{eff} \left[ \frac{\partial^2 V_r}{\partial r^2} + \frac{1}{r} \frac{\partial}{\partial r} \left( \frac{\partial V_r}{\partial r} \right) - \frac{\partial^2 V_r}{\partial z^2} \right]; \quad (83)$$

$$\rho_{eff} \frac{\partial V_z}{\partial t} + \frac{\partial V_z}{r} + \frac{\partial V_z}{\partial z} = - \frac{\partial p}{\partial z} + \mu_{eff} \left[ \frac{\partial^2 V_z}{\partial r^2} + \frac{1}{r} \frac{\partial}{\partial r} \left( \frac{\partial V_z}{\partial r} \right) - \frac{\partial^2 V_z}{\partial z^2} \right] + \rho_{eff} \beta (T - T_1); \quad (84)$$

$$\frac{\partial T}{\partial t} + \frac{\partial T}{r} + \frac{\partial T}{\partial z} = \frac{k_{eff}}{\rho_{eff} c_p} \left[ \frac{\partial^2 T}{\partial r^2} + \frac{1}{r} \frac{\partial}{\partial r} \left( \frac{\partial T}{\partial r} \right) - \frac{\partial^2 T}{\partial z^2} \right] + \frac{Q_0}{\rho_{eff} c_p}; \quad (85)$$

The boundary conditions are

$$\frac{\partial V_r}{\partial r} = 0 \text{ at } r = 0; V_z = 0 \text{ at } r = R; \frac{\partial T}{\partial r} = 0 \text{ at } r = 0; T = 0 \text{ at } r = R$$

where in the above equations  $V_r$  and  $V_z$  are defined as the components of velocity in radial and axial directions,  $T$  as the temperature of fluid,

Fig. 7. Variation of the wall shear stress distribution  $\tau_{rz}$  with  $z$  for different values of Grashof number  $Gr$  with  $\delta = 0.01, F = 0.01, d = 0.5, n = 2, \phi = 0.1, \beta = 2.0$ .

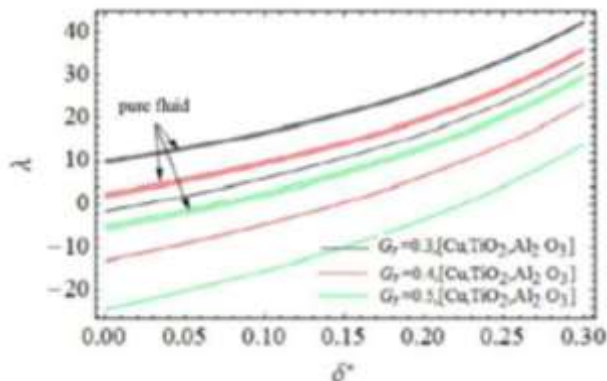


Fig. 12. Variation of resistance to flow or resistance to impedance  $\lambda$  with different values of Grashof number  $Gr$  with  $\phi = 0.01, F = 0.01, d = 0.5, n = 2, \phi = 0.1, \beta = 2.0$ .

$$\frac{\partial}{\partial z} \left[ \frac{1}{\delta(1-\phi)} \frac{\partial^2 V}{\partial r^2} \right] + \frac{1}{\delta} \frac{\partial V}{\partial r} = \frac{\delta \rho \gamma \beta}{\delta \rho \gamma \beta} Gr \theta; \quad \delta 12 \beta$$

$$\frac{\partial^2 \theta}{\partial r^2} + \frac{\partial \theta}{\partial r} = \frac{k_s + \beta 2k_f + \beta 2\phi k_f}{k_s + \beta 2k_f - 2\phi k_f - k_s} \beta \theta; \quad \delta 13 \beta$$

The non-dimensional boundary conditions on the stenosed wall are given as:

$$\begin{aligned} R_0 \leq r \leq R_0 + \delta; \quad \frac{\partial \psi}{\partial r} = 0; \quad \frac{\partial \theta}{\partial r} = 0; \quad \frac{\partial V_z}{\partial r} = 0; \quad \text{otherwise} \\ \psi = 0; \quad \theta = 0; \quad V_z = 0 \end{aligned} \quad (14)$$

$$\begin{aligned} \frac{\partial V_z}{\partial r} = 0 \text{ at } r = 0; \quad V_z = 0 \text{ at } r = R_0 + \delta \\ \frac{\partial \theta}{\partial r} = 0 \text{ at } r = 0; \quad \theta = 0 \text{ at } r = R_0 + \delta \end{aligned} \quad (15)$$

with

$$\eta = \frac{\delta}{R_0} \frac{R_0 - r}{\delta}; \quad \delta = \frac{d}{L_0}$$

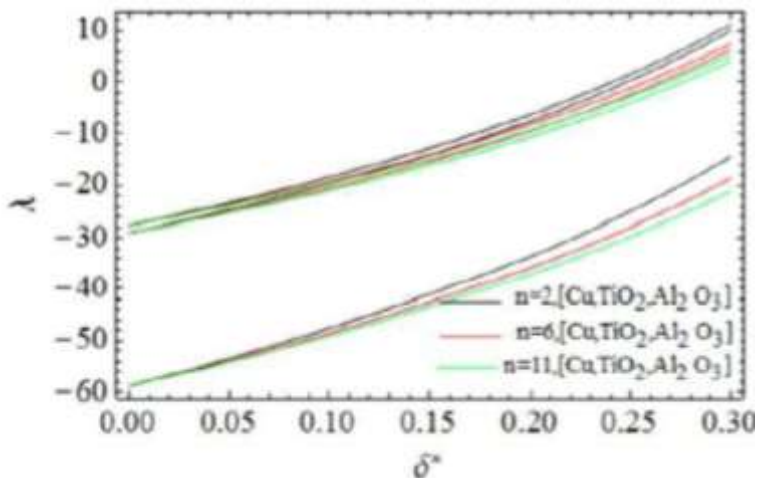


Fig. 14. Variation of resistance to flow or resistance to impedance  $\lambda$  with different values of the shape of the stenosis  $n$  with  $\varphi=0.01, F=0.01, d=0.5, Gr=0.8, \beta=2.0$ .

### Exact solutions

The exact solutions of the velocity and temperature equations using corresponding boundary conditions are directly written as

$$\frac{u}{\beta} = \frac{1}{4} \frac{d}{dz} \left[ \frac{G_0 R}{\rho_f \gamma} \frac{k_1 (1-\phi) + k_2 \phi}{k_1 (1-\phi) + 2k_2 \phi} r^2 - R^2 \right] \quad (16)$$

$$\theta = \frac{1}{4} \beta \left[ r^2 - R^2 \right] \frac{k_1 (1-\phi) + k_2 \phi}{k_1 (1-\phi) + 2k_2 \phi} \quad (17)$$

where,

$$\frac{dp}{dz} = \frac{1}{R} \frac{F}{\delta_1 - \phi} - \frac{6}{\rho_f \gamma} \frac{k_1 (1-\phi) + k_2 \phi}{k_1 (1-\phi) + 2k_2 \phi} \quad (18)$$

The corresponding stream function ( $V_z = \frac{1}{r} \frac{d\psi}{dr}$  with  $\psi=0$  at  $r=0$ ) is

$$\psi = \frac{1}{16} \frac{dp}{dz} \left[ \frac{r^2}{2} - Rr \right] + \frac{\beta}{24} \left[ \frac{r^4}{4} - 6r^2 R \right] \frac{k_1 (1-\phi) + k_2 \phi}{k_1 (1-\phi) + 2k_2 \phi} \quad (19)$$

with  $\delta^* = 0.01, d = 0.5, n = 2, z = 1.2, G_0 = 0.8, \beta = 2.0$

### Concluding remarks

The problem is concerned with the analysis of nanoparticles in the base fluid which is blood for the axisymmetric flow of nanofluid

through the artery with an axially nonsymmetric but radially symmetric mild stenosis. The effects of stenosis shape have been considered such that the axial shape of stenosis can change easily just by varying a parameter (referred to as shape parameter  $n$ ). The model studies the effect of volume fraction ( $\phi$ ), Grashof number ( $Gr$ ), heat source or sink parameter ( $\beta$ ), severity of stenosis ( $\delta^*$ ) and the flow rate ( $F$ ) for (Cu, TiO<sub>2</sub>, Al<sub>2</sub>O<sub>3</sub>), nanoparticles in the base fluid on the flow characteristics, such as the axial flow velocity, the wall shear stress and the resistance to flow.

The main finding can be summarized as follows:

- The transmission of axial velocity curves for (Al<sub>2</sub>O<sub>3</sub>) nanoparticles is higher than that of both (Cu) and (TiO<sub>2</sub>) nanoparticles at the center of the artery.
- The wall shear stress in the case of aluminum concentration (Al<sub>2</sub>O<sub>3</sub>) in the blood remains higher for both copper (Cu) and titanium (TiO<sub>2</sub>) nanoparticles.
- The resistance impedance in the case of aluminum concentration (Al<sub>2</sub>O<sub>3</sub>) in the blood remains higher for both copper (Cu) and titanium (TiO<sub>2</sub>) nanoparticles
- The trapping boluses in the case of aluminum concentration (Al<sub>2</sub>O<sub>3</sub>) are smaller than the trapping boluses for both copper (Cu) and titanium (TiO<sub>2</sub>) nanoparticles.
- The trapping boluses in the case of pure fluid ( $\phi=0$ ) reduces and trapping boluses for nanofluid ( $\phi \neq 0$ ) develop.

## References

- [1] F.D. Young, F.Y. Tsai, Flow characteristics in model of arterial stenosis steady flow, *J. Biomech.* 6 (1973) 395–410.
- [2] S. Cavalcanti, Hemodynamics of an artery with mild stenosis, *J. Biomech.* 28 (1995) 387–399.
- [3] M. Texon, A hemodynamic concept of atherosclerosis with particular reference to coronary occlusion, *Arch. Intern. Med.* 99 (1957) 418–430.
- [4] B. Liu, B.D. Tang, A numerical simulation of viscous flows in collapsible tubes with stenosis, *Appl. Numer. Math.* 32 (2000) 87–101.
- [5] J.M. Siegel, C.P. Markou, S.R. Hanson, A scaling law for wall shear rate through an arterial stenosis, *J. Biomech. Eng.* 116 (1994) 446–451.
- [6] M. Zamir, *The Physics of Coronary Blood Flow*, Springer, New York, 2005.

- [7] S. Nadeem, N.S. Akbar, Influence of heat and chemical reactions on Walter's B fluid model for blood flow through a tapered artery, *Taiwan Inst. Chem. Eng.* 42 (2011) 67–75.
- [8] K.S. Mekheimer, M.H. Haroun, M.A. Elkot, Influence of heat and chemical reactions on blood flow through an anisotropically tapered elastic arteries with overlapping stenosis, *Appl. Math. Inf. Sci.* 6 (2012) 281–292.
- [9] S. Nadeem, N.S. Akbar, Power law fluid model for blood flow through a tapered artery with stenosis, *Appl. Math. Comput.* 217 (2011) 7108–7166.
- [10] R. Ellahi, S.U. Rahman, M.M. Gulzar, S. Nadeem, K.Vafai, A mathematical study of non-Newtonian micropolar fluid in arterial blood flow through composite stenosis, *Appl. Math. Inf. Sci.* 4 (2014) 1567–1573.
- [11] K.S. Mekheimer, M.A. El Kot, The micropolar fluid model for blood flow through a tapered artery with a stenosis, *Acta Mech. Sinica* 24 (2008) 637–644.
- [12] D.S. Sankar, U. Lee, Mathematical modelling of pulsatile flow of non-Newtonian fluid in stenosed arteries, *Commun. Nonlinear Sci. Numer. Simul.* 14 (2009) 2971–2981.
- [13] R. Ellahi, S.U. Rahman, S. Nadeem, Blood flow of Jeffrey fluid in a catheterized tapered artery with the suspension of nanoparticles, *Phys. Lett. A* 378 (2014) 2973–2980.
- [14] R. Feynman, There's plenty of room at the bottom, *Science* 254 (1991) 1300–1301.
- [15] T. Hayat, T. Muhammad, A. Alsaedi, M.S. Alhuthali, Magnetohydrodynamic three-dimensional flow of viscoelastic nanofluid in the presence of nonlinear thermal radiation, *J. Magn. Magn. Mater.* 385 (2015) 222–229.
- [16] M. Sheikholeslami, R. Ellahi, R.H. Ashorynejad, G. Domairry, T. Hayat, Effects of heat transfer in flow of nanofluids over a permeable stretching wall in a porous medium, *Comput. Theor. Nanosci.* 11 (2) (2014) 486–496.
- [17] M. Sheikholeslami, R. Ellahi, M.G. Bandyopadhyay, A. Zeshni, Simulation of CuO–water nanofluid flow and convective heat transfer considering Lorentz forces, *J. Magn. Magn. Mater.* 369 (2014) 69–80.
- [18] A. Zeeshan, R. Ellahi, M. Hassan, Magnetohydrodynamic flow of water/ethylene glycol based nanofluids with natural convection through porous medium, *Eur. Phys. J. Plus* 129 (2014) 261.
- [19] V.R. Ravishankar, A.B. Jamuna, Nanoparticles and Their Potential Application as Antimicrobials. *Science Against Microbial Pathogens: Communicating Current Research and Technological Advances*, 2011.
- [20] R. Guogang, H. Dawei, W.C. Eileen, B. Cheng, A. Miguel, C. Vargas-Reus, R. Paul, P.
- [21] N.G. Chorianopoulos, D.S. Tsoukleris, E.Z. Panagou, P. Falaras, G.J.E. Nychas, Use of titanium dioxide (TiO<sub>2</sub>) photocatalysts as alternative means for *Listeria monocytogenes* biofilm disinfection in food processing, *Food Microbiol.* 28 (2011) 164–170.
- [22] A. Fujishima, K. Honda, Electrochemical photocatalysis of water at semiconductor electrode, *Nature* 238 (1972) 27–38.
- [23] A. Fujishima, K. Hashimoto, T. Watanabe, (TiO<sub>2</sub>) Photocatalysis: Fundamentals and Applications, BKC Inc., Japan, 1992.
- [24] C. Wei, W.Y. Lin, Z. Zainal, E. Williams, K. Zhu, A.P. Kruzic, R.L. Smith, K. Rajeshwar, Bactericidal activity of TiO<sub>2</sub> photocatalyst in aqueous media: toward a solar-assisted water disinfection system, *Environ. Sci. Technol.* 28 (1994) 934–938.